Available online at www.sciencedirect.com

ScienceDirect

www.elsevier.com/locate/jes

JES JOURNAL OF ENVIRONMENTAL SCIENCES

www.jesc.ac.cn

Water chemistry influences on long-term dissolution kinetics of CdSe/ZnS quantum dots

Pooya Paydary, Philip Larese-Casanova *

Department of Civil and Environmental Engineering, Northeastern University, Boston, MA, USA

ARTICLE INFO

Article history:
Received 10 July 2019
Received in revised form
7 November 2019
Accepted 14 November 2019
Available online 12 December 2019

Keywords:
Quantum dots
CdSe/ZnS
Dissolution kinetics
Shrinking particle model
Size exclusion chromatography
Inductively coupled plasma mass spectrometry

ABSTRACT

Widespread usage of engineered metallic quantum dots (QDs) within consumer products has evoked a need to assess their fate within environmental systems. QDs are mixed-metal nanocrystals that often include Cd^{2+} which poses a health risk as a nanocrystal or when leached into water. The goal of this work is to study the long-term metal cation leaching behavior and the factors affecting the dissolution processes of mercaptopropionic acid (MPA) capped CdSe/ZnS QDs in aphotic conditions. QD suspensions were prepared in different water conditions, and release of Zn^{2+} and Cd^{2+} cations were monitored over time by size exclusion chromatography-inductively coupled plasma-mass spectrometry. In most conditions with dissolved O_2 present, the ZnS shell degraded fairly rapidly over ~1 week, while some of the CdSe core remained up to 80 days. Additional MPA, Zn^{2+}, and Cd^{2+} temporarily delayed dissolution, indicating a moderate role for capping agent detachment and mineral solubility. The presence of H_2O_2 and the ligand ethylenediaminetetraacetate accelerated dissolution, while NOM had no kinetic effect. No dissolution of CdSe core was observed when O_2 was absent or when QDs formed aggregates at higher concentrations with O_2 present. The shrinking particle model with product layer diffusion control best describes Zn^{2+} and Cd^{2+} dissolution kinetics. The longevity of QDs in their nanocrystal form appears to be partly controlled by environmental conditions, with anoxic, aphotic environments preserving the core mineral phase, and oxidants or complexing ligands promoting shell and core mineral dissolution.

Introduction

Quantum dots (QDs) are small (4–10 nm) semiconductor nanocrystals with unique and tunable optical and electronic properties now featured in a wide array of nanotechnology-based applications, including drug delivery (Alivisatos, 2004; Ballou et al., 2004), solar energy conversion (Luque et al., 2007), and consumer electronics (Nozik, 2002). QDs also are part of the class of nanomaterials and nanocomposites with environmental technology and remediation applications (Ye et al., 2017a, 2019a; 2019b; Zhao and Chung, 2018) or with concerns on their environmental fate (Zhang et al., 2008a). QDs usually contain a semiconducting CdS, CdTe, or CdSe core which is sometimes coated with a protective ZnS shell, and at times may be surrounded by an organic capping agent which gives QDs stability in aqueous or solvent suspensions or a needed biological compatibility. With the projected market for the QD enabled products, QDs entrance to the aquatic environments seems inevitable by ways of product disposal in

* *Corresponding author*.
E-mail addresses: pooya.paydary@gmail.com (P. Paydary), p.laresecasanova@northeastern.edu (P. Larese-Casanova).
https://doi.org/10.1016/j.jes.2019.11.011

landfills or waste streams from manufacturing. Therefore, the chemical processes that cause QDs to persist or degrade in water require attention.

Upon release to the environment, QDs, like other engineered nanomaterials (Klaine et al., 2008), are expected to form aggregates (Morelli et al., 2012; Petosa et al., 2010; Quevedo and Tufenkji, 2009; Zhang et al., 2012a; Zhang et al., 2008b), get dissolved (Aldana et al., 2001; Hu et al., 2016; Li et al., 2012; Liu et al., 2012) or get up-taken by animals, plants, and microorganisms (Derfus et al., 2004; Navarro et al., 2012; Priester et al., 2009; Yang et al., 2011; Zhang et al., 2012b). In regards to dissolution in water environments, there is a need to better understand the unique reactivity QDs possess, which should be different than their naturally-occurring larger (~50 nm to several microns) metal sulfide or selenide minerals, and therefore require new models to describe reaction steps and kinetics. Specifically, QD structural properties could cause enhanced mineral phase reactivity in water compared to bulk minerals of the same phase. For one, due to being only a few nm thick, the core and shell mineral phases have lattice strain at some locations which can enhance their reactivity. Lattice mismatch between core and shell may also be the location of high energy sites with a greater probability of reactivity. QDs' semiconducting ability also causes them to oxidize S^{2-} and Se^{2-} and leach metal cations when exposed to UV or visible light, accelerating their dissolution (Ipe et al., 2005; Li et al., 2012). Contrarily, shell coatings may provide a layer of protection for the core against dissolution and prolong core solids (Hu et al., 2016). The organic capping agents provide colloidal stability (Dabbousi et al., 1997), a diffusion barrier to O_2 or other compounds (Aldana et al., 2001), and alter surface hydrophobicity or hydrophilicity which could influence reactivity. So far, new QD dissolution models have been developed only for the photodissolution mechanism (Li et al., 2012), but more dissolution models need to be evaluated for core-shell structured QDs without the influence of light but still influenced by other reactions such as oxidation by O_2.

Indeed, previous studies have examined how QD properties influence their transformations in water, with aggregation rates or photodissolution rates depending on their mineral composition, nanometer size, presence and thickness of a shell mineral, and presence and type of capping agent (Aldana et al., 2001, 2005; Li et al., 2012; Zhang et al., 2012). However, both the complex composition of QDs and the variability in natural aquatic chemistries call for more investigations into QD degradation or longevity in water, including environmental factors and the chemical processes involved in degradation or preservation. For one, aphotic QD dissolution studies have yet to progress to track full QD dissolution. In the absence of light, QD dissolution is much slower than photodissolution, and only partial dissolution of non-shelled CdSe in the dark has been observed after 2 days (Priester et al., 2009) or 8 days (Zhang et al., 2012a), indicating some CdSe stability to weathering. Dissolution experiments need to be extended to longer times to observe reaction completion, especially if a protective ZnS shell is present. Second, aphotic QD dissolution has been reported as a time profile or single end point observation, but no rate models have been applied to describe these data, nor have models been assessed over different water chemistries. Relatedly, it is still unknown whether the shell mineral must dissolve completely before any core leaching. Other studies reporting some CdSe/ZnS QD leaching (Mahendra et al., 2008; Morelli et al., 2012) focused on release of Cd^{2+} and not Zn^{2+} due to the relatively higher toxicity of Cd^{2+} (Hardman, 2006). Details on the simultaneous kinetics of both core and shell metal release are lacking, and QD stability studies should also assess shell mineral reactivity in addition to core mineral reactivity for a more complete characterization of QD degradation. Finally, aphotic dissolution studies have also tended to focus on QD behavior at relatively high concentrations, e.g. ~40–~75 ppm (Mahendra et al., 2008; Priester et al., 2009; Zhang et al., 2012a). At these concentrations, QDs were reported to aggregate rapidly (Mahendra et al., 2008; Zhang et al., 2012a), and aggregate formation may influence QD dissolution rates by limiting exposure of surface area with reactive agents. Hence, suspensions of individually dispersed QDs would be more appropriate for dissolution kinetic model evaluation.

A few studies have explored the influence of water chemistry on QD dissolution in the dark. In the absence of photochemical dissolution, QD dissolution and subsequent metals leaching could be governed by chemical processes that promote QD degradation, including capping agent sorption-desorption, shell and core mineral solubility, and mineral oxidation by dissolved oxidants (e.g. O_2). The presence of dissolved solutes that either enhance or diminish metal solubility thus should have a strong influence on rates of metal leaching. Strongly acidic and basic conditions have resulted in the rapid dissolution of CdSe and CdSe/ZnS QDs, likely due to increased Cd^{2+} and Zn^{2+} solubility (Mahendra et al., 2008). Complex formation with organic or inorganic ligands might also enhance Cd^{2+} and Zn^{2+} solubility; for example, CdSe in suspension with 4 mM citrate showed significant Cd^{2+} dissolution in 24 h, compared to insignificant Cd^{2+} release in Milli-Q water in similar time period (Priester et al., 2009). Seawater was also reported to have some Cd^{2+} dissolution enhancement compared to Milli-Q water, pointing to a metal-ligand complexation or an ionic strength effect on QD dissolution (Zhang et al., 2012a). Capping agent detachment has been shown to be a crucial first step before QD aggregation (Mulvihill et al., 2010; Siy and Bartl, 2010), and capping agent sorption-desorption equilibria might also influence metal cation dissolution rates. To the best knowledge of the authors, studies on the leaching behavior of the quantum dots and governing mechanisms in the dark are few, and more investigation is needed to better assess the stability of core-shell QDs in dark aqueous environments for extended periods of time.

The goal of this work is to study leaching behavior and governing dissolution mechanisms of the CdSe/ZnS QDs in dark conditions to better understand conditions where QDs may degrade or persist. The first objective was to evaluate dissolution kinetics of both shell Zn^{2+} and core Cd^{2+} metals according to traditional shrinking particle models. These kinetic models were chosen because they are applicable to complete dissolution of finite masses with possible diffusion limitation controls. The experiments were designed to accommodate these assumptions by studying QD

suspensions at low concentrations (1 ppm) without aggregation as in prior studies, and within quiescent conditions which might lead to diffusion barriers due to lack of vigorous stirring. The second objective was to evaluate the influence of water chemistry on Zn^{2+} and Cd^{2+} release, with a focus on probing the capping agent equilibria, mineral solubility, and oxidative dissolution as important processes in hindering or promoting QD dissolution. This work uses a systematic approach to understand dissolution mechanism of QDs in an aqueous environment in the dark (to prevent QD-produced ROS-mediated dissolution) and at low QD concentrations (to avoid aggregation effects on dissolution). QD suspensions were prepared in different water conditions, and Zn^{2+} and Cd^{2+} concentrations in both the QD and dissolved phases were monitored simultaneously for over two months. Mercaptopropionic acid (MPA) capped CdSe/ZnS QDs were selected for this study because they were commercially available and showed good colloidal stability. The effects of EDTA and excess amounts of MPA, Zn^{2+} and Cd^{2+} ions, as well as oxygen and hydrogen peroxide on QD dissolution were systematically investigated. Results obtained from this study benefits the understanding of fate and transformation of QDs in the dark and environmentally relevant low concentrations over a long period of time.

1. Materials and methods

1.1. *Quantum dots*

CdSe/ZnS QDs, stabilized with MPA, were purchased from NN-Labs (Fayetteville, AR, USA) and stored at 4°C until used. These QDs were selected because they have the often-studied composition, were inexpensive, and available in a wide range of sizes. Each experiment was initiated with a newly purchased QD vial within 10 days of arrival, though any small differences in QD vials could be responsible for small variations in QD reactivity. QDs had a nominal size of 8 nm (size range of 4–10 nm) and were provided as suspensions in water at a nominal concentration of 1.0 mg/mL with 1 mM MPA. Samples from each purchased QD suspension were dissolved in 1% HNO_3 and measured for total Zn^{2+} and total Cd^{2+} concentrations which were found to be typically 64.45 (1.0) and 162.2 mg/L (1.4 mM) respectively. Total S (1.0 mM) and total Se (0.7 mM) were quantified by ion chromatography after digesting a sample of QD suspension in H_2O_2 for 24 hr and detecting S as sulfite and sulfate and Se as selenite and selenate. All other chemicals used are reported in the Appendix.

1.2. *Analytical measurements*

All Cd^{2+} and Zn^{2+} concentrations were measured using inductively coupled plasma mass spectrometry (ICPMS) (Aurora M90, Bruker, USA). Size exclusion chromatography-inductively coupled mass spectrometry (SEC-ICPMS) was used to separate and quantify both Cd^{2+} and Zn^{2+}, present in both dissolved and QD phases, using high-pressure liquid chromatography (HPLC) (Prostar, Varian, USA) and chromatography conditions detailed previously (Paydary and Larese-casanova, 2015). SEC-ICPMS was used for all the experiments except otherwise noted, in which case centrifuge ultrafiltration was used to separate and quantify dissolved and QD phase Cd^{2+} and Zn^{2+}. For this centrifuge procedure, sample pH was readjusted to 5.5 using 1 mM MES and then samples were centrifuged for 15 min with a 10,000 r/min rate. Amicon ultra-4 centrifugal filter concentrators with ultracel 3 regenerated cellulose membranes and a nominal molecular weight cut-off of 3000 Da were used. Total Cd and Zn^{2+} concentrations in QD suspensions were also measured using ICPMS, after digesting QDs in 1% trace metal nitric acid solution. To calculate QDs concentration by centrifugation method, dissolved metal concentration was measured by ICPMS after centrifuging the mixture, and then it was subtracted from total metal concentration. Element detection was performed by monitoring 66-Zn^{+} and 114-Cd^{+} isotopes. Instrument dwell time was 10 ms. Se was not measured due to its expected concentrations being too close to the high instrument detection limits which was caused by interfering Ar–Ar dimers, even when the Ar–Ar dimers were minimized by H_2 collision gas. S was not measured because our ICPMS was not equipped with the required O_2 reaction gas.

QD fluorescence was measured in quartz cuvettes using an RF-5301 Shimadzu spectrofluorometer with an excitation wavelength of 250 nm. Dynamic light scattering (DLS) and zeta potential were measured using a particle size analyzer (90Plus, Brookhaven, USA). Transmission electron microscopy (TEM) (Jem-1010, Jeol, USA) was used to observe QD morphology before and after dissolution.

1.3. *Experiments*

QD dissolution experiments testing the influence of MPA, Zn^{2+}, Cd^{2+}, EDTA, H_2O_2, and O_2 were carried out over 50–80 days with a nominal QD concentration of 1 ppm. This QD concentration was chosen to minimize aggregation of the particles, which had been determined via DLS to occur at higher QD concentrations (>20 ppm) in preliminary experiments (data not shown), and to be ~500x greater than our instrument detection limit. Experiments were conducted at room temperature (19°C–21°C). Batch reactors were performed either at pH 7 with 1 mM MOPS buffer or at pH 4 with no buffer. The 1 ppm QD suspensions were made in 50 ml polypropylene tubes and sonicated for 10 s to break up any aggregates. 4.95 mL of the suspension was then immediately portioned out in 15 ml polypropylene falcon tubes and at this point amended with ~0.05 mL of reagents (described below) to test their influence on QD dissolution behavior. 2 ml was then pipetted into opaque plastic screw-cap HPLC vials which served as individual batch reactors. Preliminary experiments revealed no difference in QD dissolution when suspensions were in plastic or opaque glass vials. Suspension remaining in the 50 ml Falcon tubes was acidified and total metal present was measured using ICPMS. These total metal measurements were carried out in triplicate, and average results are reported. The SEC-ICPMS measurements for Zn^{2+} and Cd^{2+} were made singly for each batch reactor, and each water chemistry condition was tested singly, except for a demonstration of reproducibility for triplicate batch reactors at pH 7 (Fig. S1).

The effect of excess capping agent on QD dissolution was investigated by monitoring dissolution of QDs in the presence of 0.001, 0.01 and 0.1 mM excess MPA at pH 7 and pH 4 (the

original total MPA concentration carried over from the QD stock solution is estimated as 0.001 mM). MPA was added using aliquots of a methanolic MPA solution, and in a preliminary experiment, a blank spike of methanol alone was determined to not influence QD degradation rate. The influence of excess Zn^{2+} or Cd^{2+} was examined by additions of 1, 10, 100 and 500 ppb excess dissolved Zn^{2+} or Cd^{2+}, respectively. QD dissolution was also monitored in the presence of 0.01, 0.1 and 1 mM EDTA in experiments that tested ligand-promoted dissolution of QDs. EDTA was used as a model ligand due to its common use in mineral dissolution reactions (Lazo et al., 2017) and its strong affinity for both aqueous Zn^{2+} and Cd^{2+}. The effect of oxidants on QD dissolution was tested by exposing QD suspensions to 0.001, 0.01 and 0.1 mM H_2O_2, to $O_{2(g)}$ from the ambient air alone, and to O_2-free (anoxic) conditions. The anoxic conditions were ensured by preparing within deoxygenated (by boiling) DI water and storing QD suspensions inside an anoxic chamber with atmosphere composition of 99% nitrogen and 1% hydrogen. Identical 1 ppm QD suspensions were prepared, and one vial was sacrificed at each sampling time to avoid O_2 intrusion after auto-sampler needle puncture. At each sampling time, vials were transferred from the glove box to the ICPMS within anoxic, crimp-sealed glass vials to prevent exposure to O_2 during transport.

Each set of reactors testing one variable within HPLC vials also had a control reactor which only contained QDs with a 1 ppm nominal concentration at pH 7 or pH 4. All vials were stored in the dark and at room temperature without agitation. Zn^{2+} and Cd^{2+} concentrations in QD and dissolved phase were then measured using SEC-ICPMS by sampling from these vials over time. Vial caps were substituted after each sampling by the auto-sampler to prevent evaporation of the contents through auto-sampler puncture hole during storage. For all reactors exposed to atmospheric O_2, the dissolved O_2 concentration was assumed to be at saturation (250 μM) which is far greater than QD sulfide and selenide concentrations (~2 μM) and therefore not a limiting reactant.

The effect of natural organic matter on QD dissolution rates was also examined at 1 ppm CdSe/ZnS QDs but performed in 50 ml falcon tubes with larger volume for sample processing via centrifuge ultrafiltration. Solution pH was adjusted to 6.5, and reactors were let to sit in the presence of 0, 10 and 50 ppm NOM. Samples taken over time were first mixed with excess dissolved Zn^{2+} to a final Zn^{2+} concentration of 50 ppm and then centrifuged. Initially, Cd^{2+} and Zn^{2+} recovery in the presence of NOM was low, so 50 ppm Zn^{2+} was added to samples to get > 95% Cd recovery, presumably by out-competing Cd^{2+} for complex sites within NOM, and thus for reactors with NOM, only Cd^{2+} was measured. Cd^{2+} recovery after centrifuge ultrafiltration was also found to be > 95% only at pH 6.5 or below and not at 7.0 or above.

Experiments testing higher concentrations of QDs (20 ppm) were performed in a 100 ml glass bottle at pH 5.5 with 2 mM MES buffer, slightly more acidic than the 1 ppm batch reactors to facilitate dissolution using higher H^+ concentrations, under static conditions with occasional gentle agitation by hand. This QD nominal concentration was found to be the lowest that produced reliable hydrodynamic diameter measurements with our particle analyzer. Samples were collected over 30 days to measure dissolved Cd^{2+} and Zn^{2+} present in the suspension as well as hydrodynamic diameter, zeta potential and spectrofluorescence of the QDs. Samples collected for dissolved Cd^{2+} and Zn^{2+} were filtered by centrifuge ultrafiltration. Dissolved Cd^{2+} and Zn^{2+} were measured in the filtered liquid using ICPMS.

The experiment to assess potential toxicity of QDs before and after QD dissolution was conducted by comparing growth curves of the bacterium *E. coli* K12 under different water chemistries. *E. coli* cells were first grown in LB medium at 37°C for ~12 hr until late log growth phase. Four different conditions were prepared: LB medium alone, LB medium with 1 ppm QDs, LB medium with partially dissolved QDs (0.7 ppm QDs, 30 ppb dissolved Cd^{2+}, 24 ppb dissolved Zn^{2+}), and LB medium with dissolved QDs only (150 ppb dissolved Cd^{2+}, 68 ppb dissolved Zn^{2+}, no QDs remaining). 1.5 mL of each solution was added to cuvettes in triplicate, and 20 μL of grown cells were added to initiate the growth experiment. Control cuvettes containing no cells and only LB medium alone, LB medium with 1 ppm QDs, and LB medium with fully dissolved QDs only were also prepared. All cuvettes were stored at 37°C and measured spectrophotometrically for optical density at 600 nm over 9 hr.

2. Results and discussion

2.1. QD dissolution kinetics

Dissolution kinetics of CdSe/ZnS core-shell QDs capped with MPA were first examined in air-saturated water at pH 7 over an 80 day period to simulate long-term weathering in oxic waters without exposure to light. QD dissolution was initiated immediately with release of both Zn^{2+} and Cd^{2+} into the dissolved phase (Fig. 1). Dissolved Zn^{2+} rapidly increased early which corresponded to a sharp decrease in QD phase Zn^{2+}, with complete dissolution of the ZnS shell in less than 7 days. In contrast to Zn^{2+}, the dissolved Cd^{2+} concentrations increased more slowly, and QD phase Cd did not completely disappear even after 80 days. The initial dissolution of the ZnS shell and longer persistence of the CdSe core was confirmed using a separate stock of purchased CdSe/ZnS QDs (Fig. S1), and this experiment was conducted in triplicate identical batch reactors to demonstrate good reproducibility.

Complete Zn^{2+} and Cd^{2+} mass accountability was observed at pH 7 throughout the reaction time course in Fig. 1. The sum of Zn^{2+} and Cd^{2+} concentrations, calculated by adding the dissolved and QD phase Zn^{2+} and Cd^{2+} concentrations measured by SEC-ICPMS at each time point, were nearly constant, indicating no other reaction products formed. Furthermore, the digested total Zn^{2+} and Cd^{2+} concentrations, measured in unfiltered samples by ICPMS after acid digestion, were also constant and were within 15% of the sum of Zn^{2+} and Cd^{2+} respectively, suggesting little loss of QD or dissolved cations to reactor vial surfaces or the SEC column during analysis. Good recovery and mass balance agreements were also observed for Zn^{2+} and Cd^{2+} in an identical batch reactor conducted at pH 4 (Fig. S2).

The Cd dissolution kinetics appeared biphasic, with a rapid leaching early when the ZnS shell was still present followed

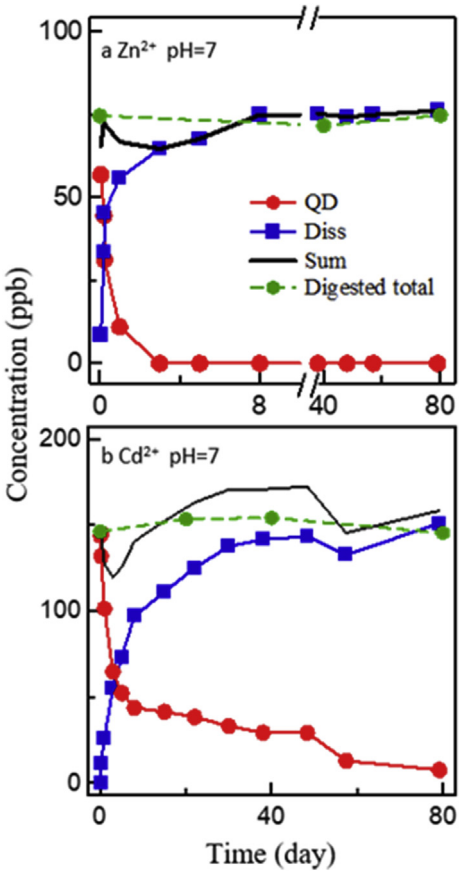

Fig. 1 – Dissolution of CdSe/ZnS quantum dots (QDs), nominal concentration of 1 ppm, at pH 7 over time. Sums of dissolved and QD phase metal concentrations measured by size exclusion chromatography inductively coupled plasma (SEC-ICPMS) are noted as "Sum Zn" and "Sum Cd". Digested total metals refers to metals concentrations after acid digestion and measurement by ICPMS.

by a slower release. The simultaneous release of Zn^{2+} and Cd^{2+} early could indicate that ZnS shell was not a uniform and closed layer but rather a non-uniform layer with crevasses that expose Cd core. These crevasses likely initially formed during QD synthesis when growing ZnS islands met (Van Sark et al., 2001). TEM images (Fig. 2) showed that fresh QDs are in fact not uniform spheres but instead angular which could result in non-uniform ZnS coverage and making them prone to non-uniform ZnS dissolution and early CdSe core exposure. The angular shape could also produce regions with different CdSe or ZnS lattice strains and consequently different reactivities. Early exposure, a higher CdSe lattice strain, and the lattice mismatch with ZnS for the outer CdSe layers could together explain the initial rapid leaching of Cd, and a more structurally homogenous inner CdSe core could provide some stability and consequently a slower leaching rate in later days. Additional TEM images confirmed a generally smaller size of remaining QDs after aging, and a far fewer number of QDs after aging were able to be imaged at all (Fig. S3). This indicates that QDs reactivity may vary among similar nanoparticles, with some fast dissolving QDs contributing to the initial Cd release. Early Cd^{2+} leaching is important because it has been

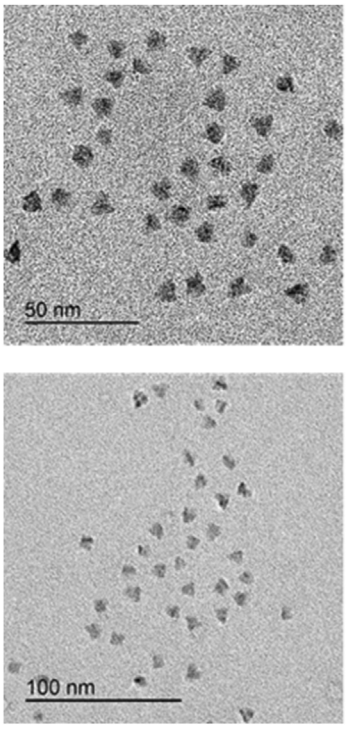

Fig. 2 – TEM images of mercaptoproprionic acid (MPA)-capped CdSe/ZnS QDs.

previously reported that cytotoxicity of the QDs correlates with the release of free Cd^{2+} ions due to degradation of the CdSe crystal and when appropriately coated, CdSe-core QDs are nontoxic (Derfus et al., 2004; Mahendra et al., 2008). On the other hand, CdSe core persistence in the dark, even in the absence of ZnS shell, gives QDs significant time for movement and exposure to aquatic life as a nanoparticle.

The QD dissolution kinetics is likely influenced by a variety of interfacial processes that can act simultaneously on and within the complex core-shell structure of the dual reduced minerals. To the best of the authors' knowledge there has been no study on the dissolution kinetics of CdSe/ZnS QDs without light in air-saturated water for low QD concentrations (devoid of QD aggregation) and for both shell and core metals. Under such conditions, QD dissolution is assumed to be driven by oxidation of S^{2-} and Se^{2-} by O_2, and by mineral solubility (Habashi, 1966; Zeng et al., 2015). To better understand the physicochemical factors that can influence QD dissolution rates in addition to structural inhomogeneity described above, kinetic modeling was performed to evaluate the relative importance of mass transfer processes and surface reaction processes, one of which is typically rate-limiting for mineral dissolution reactions.

Diffusion of O_2 to the QD surface or diffusion of metal cations away from the surface might be an important mass transfer process considering the static hydrodynamic nature of the batch reactors without stirring and the MPA and ZnS coatings over the CdSe core. The kinetic models for shrinking particles in fluids (Levenspiel, 1999) were chosen because they can account for complete disappearance of the QD phase where reactive surface area decreases over time as atomic layers dissolve away, instead of assuming an infinite solid

present. These models have been applied previously to describe the oxidative dissolution of ZnS under different reactant and mass transfer regimes (Aydogan, 2006; Ghassa et al., 2017). When only diffusion of atoms (e.g., O_2) across the thin film at the solid-water interface (such as the diffuse double layer) limits the reaction rate, the kinetics can be described as.

$$1-(1-X)^{2/3}=k_d t \quad (1)$$

where, k_d (day^{-1}) is the thin film diffusion controlled rate coefficient, t (day) is time, and X is the fraction reacted. When diffusion through a buildup of a porous product layer limits the reaction rate, the kinetics can be described as.

$$1-3(1-X)^{2/3}+2(1-X)=k_p t \quad (2)$$

where k_p (day^{-1}) is the product layer diffusion controlled rate coefficient. Should only the surface reaction limit the overall reaction rate, the kinetics can be described as.

$$1-(1-X)^{1/3}=k_r t \quad (3)$$

where k_r (day^{-1}) is the reaction controlled rate coefficient.

The most appropriate kinetic model to describe QD dissolution should provide the best linear relationship between the left-hand side of the equation and t, with the rate coefficient as the slope. Of all three models, the product layer diffusion control model (Eq. (2)) consistently fit dissolution data for both Zn^{2+} and Cd^{2+} from Fig. 1 and Fig. S1 (Fig. 3) and typically held superior correlation coefficient (R^2) values (Table 1). R^2 values for equation (2) were all >0.90, whereas those values for the other models were typically less and sporadic, although for two replicates from Fig. S1 values across all models were nearly identical for Cd. These replicates, though, had only 4 or 5 data points for Cd compared to Cd in Fig. 1 which had 9 points and a stronger correlation. Hence, the release of both Zn^{2+} and Cd^{2+} can be considered to be acting under some diffusion limitation but not far from being controlled by the surface reaction. Note that Cd data in Fig. 3 were fit up to near the first 38 days of dissolution only, with later data deviating from the model (not shown). This indicates that about the first 90% of Cd dissolution could be described with a diffusion limitation, but remaining CdSe cores were somehow more resistant to dissolution and subjected to other physicochemical controls. Furthermore, the modeling procedure for Cd eliminated the first several sampling points that showed no Cd leaching and reset the time in Fig. 3 to the first sampling point with dissolved Cd, thereby eliminating the lag time in Cd dissolution which the model does not account for.

The product layer diffusion controlled rate coefficients k_p for Cd^{2+} and Zn^{2+} were generally on the same order of magnitude, with slightly higher values for Zn^{2+} (Table 1). The ZnS phase may be more reactive compared to CdSe considering the structural inhomogeneity described above. k_p values for Cd were remarkably consistent, but values for Zn^{2+} reflect different reactivities among reactors which could be caused by QD aging during storage.

Table 1 – Linear correlation coefficients (R^2) for kinetic models in equations (1)–(3), and reaction rate coefficients for equation (2), for Zn^{2+} and Cd^{2+} dissolution kinetic profiles presented in Fig. 1 and Fig. S1, and modeled in Fig. 3.

	Thin film diffusion	Product layer diffusion*	Surface reaction	k_p (day^{-1})	n **
	R^2	R^2	R^2		
Zn^{2+} dissolution					
Fig. 1	0.47	0.98	0.90	0.440	4
Fig. S1	−0.15	0.95	0.52	0.022	8
	0.42	0.95	0.70	0.020	8
	0.22	0.92	0.48	0.023	8
Cd^{2+} dissolution					
Fig. 1	0.72	0.99	0.87	0.019	9
Fig. S1	0.67	0.95	0.66	0.019	4
	0.93	0.90	0.94	0.017	5
	0.92	0.90	0.91	0.017	4

* fitted data for the product layer diffusion controlled model appear in Fig. 3. Fitted data for the other two models are not included; ** n = number of fitted data points.

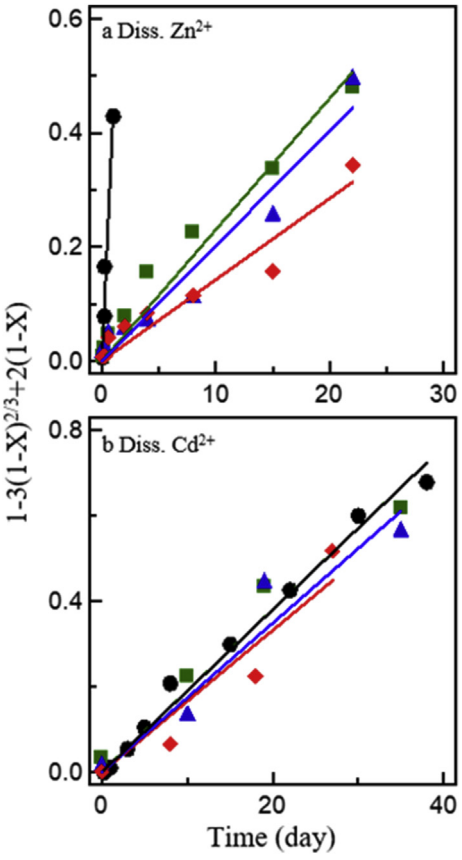

Fig. 3 – Zn^{2+} and Cd^{2+} dissolution kinetics from Fig. 1 and Fig. S1 modeled with the product layer diffusion control model (equation (2)). Zn^{2+} data was modeled until complete dissolution, and Cd data was modeled with day 0 as the start of Cd^{2+} dissolution, which occurred between actual days 1 and 22. Markers represent four experiments: black circles represent data from Fig. 1, and the green squares, blue triangles, and red diamonds represent triplicate reactors from Fig. S1.

These observations point to an influence of a product layer building up on the QD surface for most of the QD lifetime, leading to a slowing of O_2 access or Cd^{2+} or Zn^{2+} release. This product layer could be a combination of physical barriers such as residual MPA and ZnS layers, the distance to diffuse through atom-layer crevasses or pores (Van Sark et al., 2001), or the accumulation of insoluble S^0, Se^0, or metal oxide oxidation products. For example, others have reported the capping agent chain length can influence O_2 diffusion and control photooxidation rates (Aldana et al., 2001). CdSe/ZnS oxidation has been observed to form the oxides CdO and ZnO as measured by XPS (Pechstedt et al., 2010). Others (Durisic et al., 2011) proposed CdSe/ZnS photodegradation created a sulfur-rich layer composed of S^0 or polysulfides that inhibited ZnS and CdSe dissolution by blocking O_2 access. A buildup of a S^0 enriched layer has also been reported after bulk ZnS oxidation (Acero et al., 2007). Complete QD dissolution may then be achieved after slow dissolution of S phases to sulfur oxyanions. In the present study, dissolved and solid phase S, Se, or metal oxide species were not identified or quantified due to low amounts. Finally, the role of ion accumulation at QD surfaces has been proposed to influence reaction rates. The kinetics of photochemical dissolution of CdSe/ZnS, which also showed a parabolic profile and incomplete dissolution of Cd, were described with a pseudo-first order model that included an assumption that the known total mass of QDs was not entirely available for dissolution (Li et al., 2012). Instead, a quasi-equilibrium condition was suggested to exist between near-surface dissolved ions and the QDs, and these ions block the diffusion of reactants to the QD cores and minimize the available surface area for reaction.

The possibility of near-surface dissolved metal cations slowing QD dissolution rates is also supported by the fact that dissolved ions in equilibrium with nanocrystals provide the most thermodynamically stable state (Siy and Bartl, 2010). Therefore, water chemistry may hold conditions (specifically, the presence of excess dissolved solutes) that shift equilibrium to preserve rather than dissolve the QD phase. To more accurately probe the release of metal cations from QDs, dissolution behavior needs to be evaluated under the influence of these processes including acid dissociation equilibria, capping agent sorption-desorption equilibria, and metal cation dissolution-precipitation equilibria. Their relationship to QD oxidation rates during long-term dissolution are explored in the sections below.

2.2. *Influence of MPA concentration*

Thiol capping agent dissociation from the shell surface is thought to be the first step in QD dissolution (Aldana et al., 2005; Mulvihill et al., 2010). Short chain (C2–C6) capping agents such as MPA (C4) are particularly unstable on the QD surface and can readily detach, even at neutral pH values (Mulvihill et al., 2010). The addition of excess MPA might slow degradation by providing replacement capping agents or by improving the driving force for MPA sorption to the surface, preserving the ZnS shell. The possible role of capping agent sorption-desorption equilibria in slowing QD dissolution rates was therefore examined. CdSe/ZnS-MPA QDs at pH 7 showed no change in Zn^{2+} or Cd^{2+} dissolution rates when excess MPA was added up to 0.1 mM (Fig. S4). It is possible the as-received QDs were already saturated with surface MPA and added MPA did little to promote more attachment at any point during dissolution. A likely explanation also could be the prevention of dissolved MPA to adsorb due to electrostatic repulsion with sorbed MPA. At pH 7, MPA carboxyl groups are negatively charged (pKa = 4.35), and the repulsion of similar charges between dissolved MPA and QD bound MPA might inhibit MPA sorption and bonding with available surface Zn^{2+}.

To better observe any effect of MPA sorption-desorption dynamics on QD degradation, a second dissolution experiment was conducted at pH 4 to contain mostly neutral MPA species and remove the possibility of electrostatic repulsion. First, at pH 4 without any additional MPA, the ZnS shell completely dissolved before the first data point was measured (<15 min), while the CdSe core persisted over 15 days. Comparing the reaction profiles for QDs alone in Fig. 1 (pH 7) and Fig. 3 (pH 4) indicates that the presence of a higher concentration of H^+ increased the QD dissolution rate. More acidic conditions have been shown elsewhere to result in greater dissolution extent for CdSe/ZnS QDs (Mahendra et al., 2008; Slaveykova and Startchev, 2009) as well as for bulk ZnS (Acero et al., 2007). It has been shown previously that when the H^+ concentration at the interface of the QD and the capping agent increases, H^+ may out-compete the surface cation for the thiol group of the capping agent (pKa ~10.5) and cause dissociation of the nanocrystal surface-capping agent bond and the release (Aldana et al., 2005; Mandai and Tamai, 2008; Zhang et al., 2008b), leading to increased exposure of surface sites. Higher H^+ concentrations also provide more thermodynamically favorable conditions for H_2S (pKa 7.1) and H_2Se formation (pKa 3.9) which can increase chalcogenide solubility (Habashi, 1966; Zeng et al., 2015). The odor of H_2S or H_2Se gases were noticed over time in our preliminary experiments when pH was lowered to 3 (data not shown). The faster shell ZnS dissolution can also be explained by a faster inherent oxidation kinetics of ZnS with O_2 at lower pH (Acero et al., 2007).

At pH 4 with excess MPA added, QDs dissolution was suppressed (Fig. 4). 0.001 mM of MPA slightly slowed the release of dissolved Zn^{2+} and Cd^{2+}, while MPA concentrations of 0.01 and 0.1 mM slowed down the dissolution process significantly. The 0.01 and 0.1 mM of dissolved MPA resulted in almost the same dissolution kinetic profiles, suggesting that there might be an upper limit to which QDs dissolution can be suppressed by excess MPA, such as achieving a surface site saturation. Improved QD resistance to dissolution in the presence of excess capping agent at pH 4 can be explained by the dynamic nature of dissociation and re-coordination of the capping ligands on the QD surface. It is well known that there is a dynamic sorption-desorption equilibrium between free capping agents in the solution and capping ligands on the QD surface (Parak et al., 2003; Green, 2010; Mulvihill et al., 2010; Siy and Bartl, 2010; Hu et al., 2016). Excess dissolved capping agent has also been shown to preserve CdSe-MPA QD colloidal stability and prevent aggregation over 20 hr (Mulvihill et al., 2010), as well as slow CdSe-MPA photodegradation by replacing surface-oxidized MPA (Aldana et al., 2001). For CdSe/ZnS-MPA QDs here oxidized by O_2 at pH 4, the rapid dissolution could likewise possibly be slowed by MPA reattachment

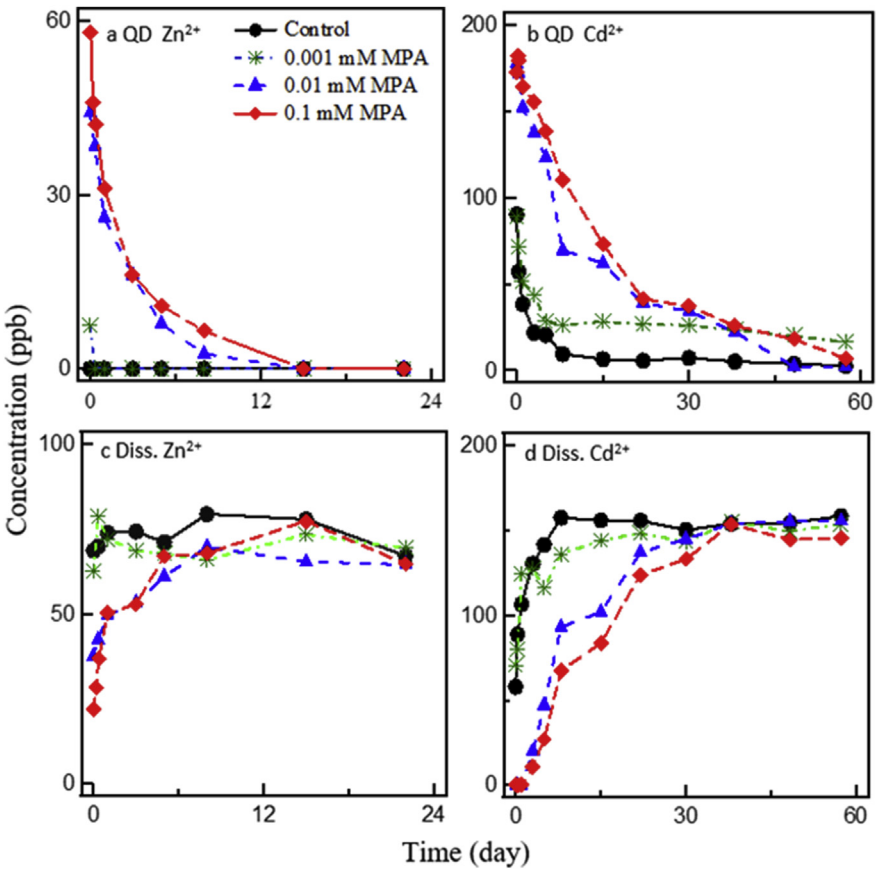

Fig. 4 – Influence of excess MPA (0, 0.001, 0.01, or 0.1 mM) on dissolution kinetics of MPA-capped CdSe/ZnS QDs at pH 4. (a) Zn^{2+} in the QD phase, (b) Cd^{2+} concentrations in the QD phase, (c) dissolved Zn^{2+} concentrations, and (d) dissolved Cd^{2+} concentrations.

onto ZnS or CdSe surfaces. Moreover, the continued presence of an MPA layer might slow diffusion of O_2 and leached cations. Diffusion limitation of O_2 and oxidation products through MPA chains in the early stages of photo-degradation has been previously observed (Aldana et al., 2001). These diffusion processes could be further demonstrated in QD dissolution experiments that expose QDs to longer chain capping agents, and slower dissolution kinetics could be caused by slower O_2 diffusion through the attaching longer chains. Overall, the capping agent sorption equilibria process may slow QD dissolution, and if excess capping agent coexists with QDs released into nature, QD in their nanocrystal form may have more longevity.

2.3. *Influence of added Zn^{2+} and Cd^{2+}*

It is possible QDs would coexist with their dissolved metal cations should metals in both phases be released from products, found co-occurring in waste streams, or QDs partially dissolve. Others have also hypothesized metal cations and metal-sulfide precursor molecules should associate with QD surfaces (Li et al., 2012). Consequently the presence of excess dissolved Zn^{2+} or Cd^{2+} on QD dissolution kinetics was examined to determine the effect, if any, these cations have on preserving QDs by lowering mineral phase solubility. Excess dissolved Zn^{2+} prolongs the ZnS shell and CdSe core when Zn^{2+} concentrations are greater than 1 ppm (Fig. 4a–c). A delay in the onset of ZnS dissolution was observed at the higher Zn^{2+} concentrations, but ZnS disappearance proceeded at nearly the same rate as indicated by similar linearly decreasing slopes. This suggests that ZnS preservation by Zn^{2+} is temporary and that oxidation by O_2 at the ZnS surface eventually predominates.

The additional Zn^{2+} likely slowed down QD dissolution by limiting ZnS shell solubility. Excess dissolved Zn^{2+} has been shown to decrease initial rates of non-oxidative dissolution of ZnS (Crundwell and Verbaan, 1987) due to diminished solubility via the common ion effect. To estimate changes in solubility with water chemistry, thermodynamic modeling of dissolution-precipitation equilibria was performed with visual MINTEQ (Gustafsson, 2018) by modeling the QD as two separate ZnS (1.0 μM as sphalerite) and CdSe (1.4 μM) solid phases corresponding to the total initial Zn^{2+} and Cd^{2+} μM concentrations present in the batch reactors. Without any added Zn^{2+} and without oxidation by O_2, about 0.2% of Zn^{2+} is expected to dissolve at pH 7, and the addition of any amount of dissolved Zn^{2+} leads to complete suppression of ZnS dissolution. Thus, the excess Zn^{2+} likely temporarily suppressed the tendency of solid Zn^{2+} to flee to the aqueous phase. This ZnS preservation also can explain the lag in CdSe core dissolution by delaying CdSe sites being exposed to water. Thermodynamic modeling did not predict any

significant formation of ZnSe solid, so Zn^{2+} substitution into the CdSe phase was not considered a likely influence on CdSe degradation rates.

The addition of excess Cd^{2+} clearly slowed the release of Zn^{2+} from the shell but had almost no effect on the release of Cd^{2+} from the core (Fig. 5d–f). Increasing concentrations of dissolved Cd^{2+} delayed the onset of Zn^{2+} release by a few days and also slightly decreased the rate of Zn^{2+} release. The addition of 50 ppm Cd^{2+} prolonged the ZnS phase until 50 days, whereas the ZnS shell disappeared after 30 days with no additional Cd^{2+}. This temporary hindrance is attributed to the possible doping of Cd, or even the formation of a secondary CdS phase, upon cation substitution of Cd for Zn^{2+} in the ZnS shell. Thermodynamic modeling predicted that, at equilibrium, any added Cd^{2+} would form CdS (modeled as greenockite due to being isostructural with sphalerite). Cation substitution of Pb^{2+} into CdS has been observed (Hsieh et al., 1993) albeit under anoxic conditions only. Thus it is possible any formation of CdS could alter, and in this case slow, the reactivity of shell ZnS with O_2. Core CdSe dissolution profiles, though, were nearly identical. At equilibrium without any O_2, CdSe is not expected to dissolve Cd to any measurable amount, whether excess dissolved Cd^{2+} is present or not. Excess Cd^{2+} therefore had no influence on the already poorly soluble CdSe at pH 7. The process of suppressing mineral solubility with excess dissolved cations

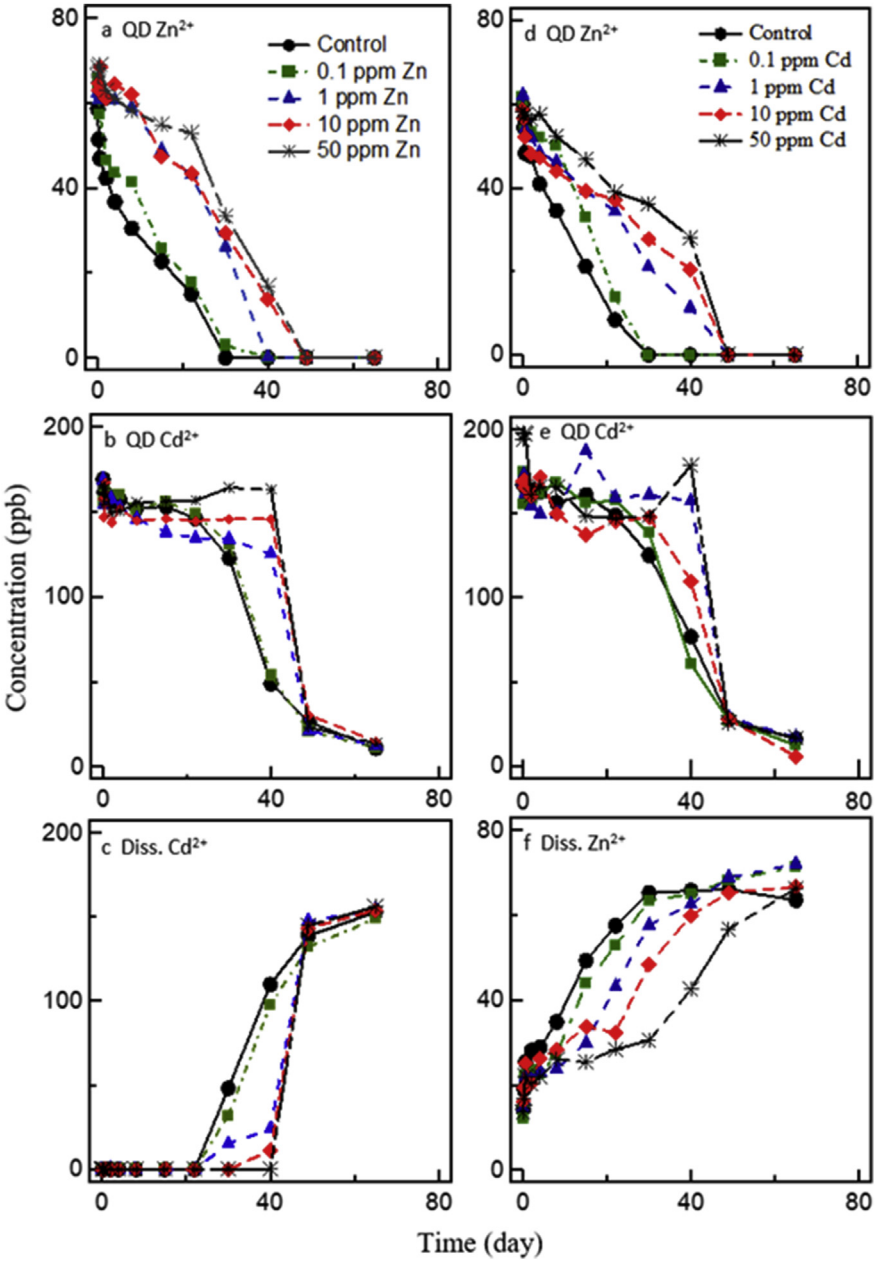

Fig. 5 – Influence of excess Zn^{2+} (a, b, c) and excess Cd^{2+} (d, e, f) on dissolution kinetics of CdSe/ZnS QDs at pH 7. 0.1, 1, 10, and 50 ppm Zn^{2+} correspond to 1.5, 15, 150, and 750 μM, and 0.1, 1, 10, and 50 ppm Zn^{2+} correspond to 0.9, 9, 90, and 450 μM.

appears to have only a minor influence on QD dissolution rates.

2.4. *Influence of oxidants*

Oxygen molecules can readily oxidize selenides and sulfides in semiconducting nanocrystals (Spanhel et al., 1987; Alivisatos, 1996), and in the case of CdSe it has been shown that oxidation produces selenium oxyanions that can detach from the QD surface and leave behind Cd^{2+} cations (Derfus et al., 2004; Zeng et al., 2015). Oxidative dissolution by O_2 is likely the primary pathway of QD dissolution in oxic waters, but oxidation by ROS could be a possible transformation route as well. Reactive oxygen species can be generated photochemically by light irradiation of QDs with O_2 present (Ipe et al., 2005; Pechstedt et al., 2010; Li et al., 2012; Wu et al., 2014) or by irradiation of NOM (Fujii and Otani, 2017) which potentially form superoxide, hydrogen peroxide, and hydroxyl radicals. QDs could therefore be exposed to a spectrum of oxic to anoxic conditions and a variety of oxidants in natural waters. Oxidative dissolution of CdSe/ZnS-MPA QDs in dark and in the absence and presence of O_2 and H_2O_2 was investigated with the hypothesis that greater abundance of oxidants should promote QD degradation.

The role of O_2 in facilitating QD dissolution was first confirmed in two batch reactors comparing QD dissolution rates in oxic versus anoxic conditions (Fig. 6). In anoxic conditions, about half of the ZnS shell dissolved over the experimental period while dissolution of the CdSe core was completely halted. The Zn^{2+} release should be due to some QD dissolving to achieve an equilibrium with dissolved Zn^{2+} and sulfide species (H_2S, HS^-, S^{2-}), but oxidation by trace remaining O_2 is also possible. The 50% dissolution of ZnS is far greater than the 0.2% dissolution predicted with thermodynamic modeling which supports the notion of either trace oxidation or a lower solubility product constant for the ZnS shell. The lack of any CdSe core dissolution could be due to protection by remaining ZnS shell but is also consistent with thermodynamic equilibrium predictions of <0.01% of 1.4 μM CdSe dissolving at pH 7 in anoxic water. These observations suggest that in oxic conditions dissolution of CdSe is mainly derived by oxidation of Se^{2-}, and in anoxic conditions CdSe may survive for extended periods of time. Oxygen molecules can readily oxidize selenides and sulfides in semiconducting nanocrystals (Spanhel et al., 1987; Alivisatos, 1996), and in the case of CdSe it has been shown that oxidation produces selenium oxyanions that can detach from the QD surface and leave behind Cd^{2+} cations (Derfus et al., 2004; Zeng et al., 2015).

H_2O_2 was chosen as an oxidant because not only it is reported to be the intermediate oxidant in photodegradation of QDs (Li et al., 2012), but it is a relatively stable ROS and found naturally in surface waters at high nanomolar to low micromolar concentrations (Cooper et al., 1988; Cooper and Lean, 1989). The presence of H_2O_2 accelerated QD dissolution rates in oxic conditions. 0.01 and 0.1 mM H_2O_2 concentrations only moderately improved ZnS and CdSe dissolution rates compared to O_2 alone. ZnS dissolution was complete, though, at the same time (30 days) for ZnS under all three conditions. The onset of CdSe dissolution occurred earlier at higher H_2O_2 concentrations until day 30, but for days 30–48 CdSe dissolution rates were identical. This indicates that these amounts of H_2O_2 were sufficient to promote oxidative dissolution of the 1.0 μM of ZnS and some of the 1.4 μM of CdSe, but by day 30 may have decayed by reaction with QDs or by autodecomposition. H_2O_2 concentrations up to approximately 100 times greater than the sulfide and selenide concentrations therefore only moderately increased QD degradation rates. This indicates that natural waters with about 1 μM H_2O_2 might have little influence on QDs at micromolar concentrations of S^{2-} and Se^{2-} but perhaps a more significant influence for lower, nanomolar concentrations of S^{2-} and Se^{2-}. With approximately 1000 fold greater H_2O_2 compared to S^{2-} and Se^{2-} concentration (the 1 mM H_2O_2 condition), QD dissolution was rapid with complete Zn^{2+} and Cd^{2+} release after 3 and 15 days, respectively. The anoxic and oxic dissolution results indicate that oxidative dissolution should be the primary process of QD degradation in nature, and mineral solubility plays a lesser role.

Kinetic modeling was also performed to check for any changes in reaction controls subjected to H_2O_2 (Table S1). Of all three kinetic models, the dissolution data for Zn^{2+} was still best fit with the product layer diffusion control model, even in the presence of highest H_2O_2 concentrations, similar to what was previously observed at section 2.1. For Cd^{2+} data, all three models resulted in almost the same R^2 values leaving the primary control unidentifiable. The product layer diffusion controlled rate coefficients k_p for Cd^{2+} and Zn^{2+} in the presence of 0, 0.01, and 0.1 mM H_2O_2 were generally on the same order of magnitude as those without H_2O_2 in Table 1 and 1 mM H_2O_2 resulted in a factor of 10- to 20-fold higher rate coefficients.

2.5. *Influence of complexing ligands*

2.5.1. *EDTA*

In contrast to excess Zn^{2+} and Cd^{2+} which can suppress QD solubility and dissolution rates, organic ligands were added to QD suspensions to examine if increasing metal solubility increases dissolution rates. The process of ligand-promoted dissolution involves the coordination of a surface metal cation with a complexing ligand, weakening nanoparticles structural bonds, and allowing the molecules to desorb. This process has been previously stated to be an important mechanism in destabilizing nanoparticles in natural aqueous systems (Slaveykova and Startchev, 2009; Navarro et al., 2010; Li et al., 2012; Quigg et al., 2013; Chang and Waclawik, 2014). Low molecular weight organic ligands found in natural waters include organic acids (Vančura and Hovadík, 1965), phytosiderophores (Marschner et al., 1986), and siderophores (Hider and Kong, 2010), as well as synthetic EDTA by introduction from wastewaters. Here, EDTA was used as a model ligand due to its common use in mineral dissolution reactions (Lazo et al., 2017) and its strong affinity for both aqueous Zn^{2+} and Cd^{2+}.

Accelerated dissolution of the QDs was observed in the presence of 0.01, 0.1, and 1.0 mM EDTA (Fig. 7). These EDTA concentrations were chosen because thermodynamic equilibrium modeling predicts complete dissolution for only $ZnS_{(s)}$ (as bulk sphalerite) and <1% dissolution for bulk $CdSe_{(s)}$ at all EDTA concentrations, and so EDTA might influence the two

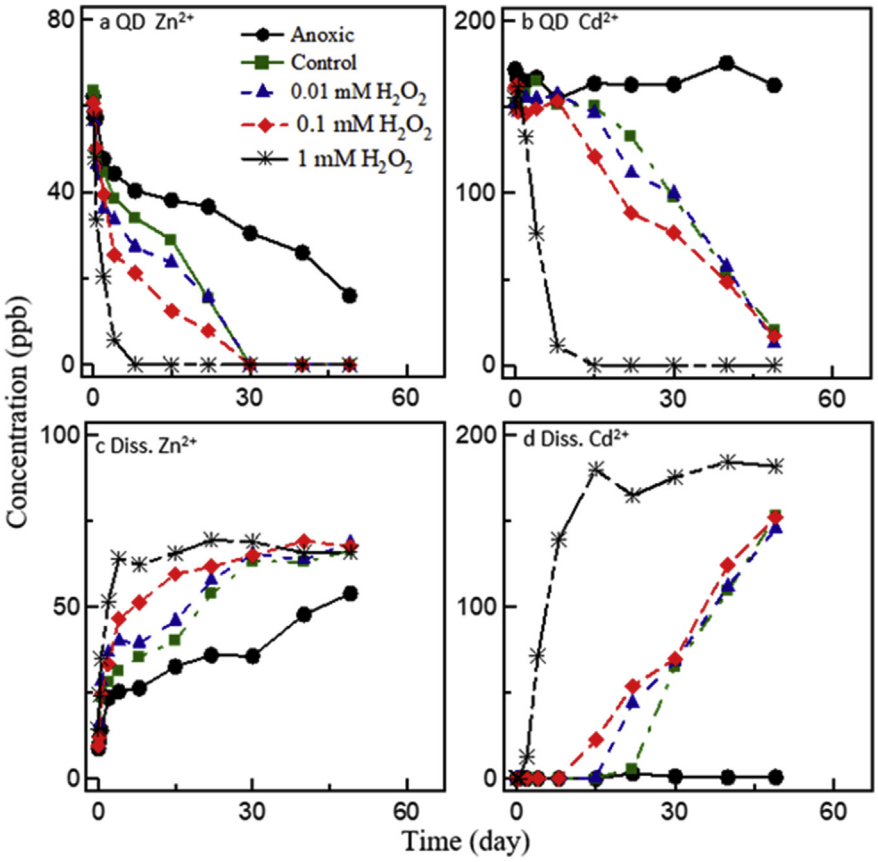

Fig. 6 – Influence of added H_2O_2 (0, 0.01, 0.1, or 1 mM) and the presence vs. absence of O_2 on dissolution kinetics of CdSe/ZnS QDs at pH 7. (a) Zn^{2+} in the QD phase, (b) Cd^{2+} concentrations in the QD phase, (c) dissolved Zn^{2+} concentrations, and (d) dissolved Cd^{2+} concentrations.

mineral phases to different extents. First, the dissolved Zn^{2+} and Cd^{2+} profiles were identical across all EDTA concentrations due to EDTA added in excess of Zn^{2+} (1.0 μM) and Cd^{2+} (1.4 μM) and therefore not a limiting reactant. The ZnS shell was completely dissolved within 24 h for all EDTA concentrations, whereas 30 days were required when no EDTA was provided. The short $ZnS_{(s)}$ lifetime suggests metal-ligand complexation was a faster process compared to oxidative dissolution. Cd^{2+} was also rapidly released with EDTA, although a small amount of the core $CdSe_{(s)}$ still required up to 40 days for complete dissolution. The rapid initial Cd^{2+} dissolution over the first few days could be due to EDTA complexation of Cd^{2+} from more reactive, high-energy surface sites more readily dissolvable compared to bulk $CdSe_{(s)}$. Relatedly, others have reported ZnS solubility, in the presence of EDTA, at the nanoscale increases several orders of magnitude compared to bulk ZnS due to particle size effects (Zhang et al., 2010). The second slower dissolution step could be explained by a more robust $CdSe_{(s)}$ core whose dissolution is less influenced by metal-ligand complexation (as predicted by equilibrium modeling) and more governed by Se^{2-} oxidation. Although EDTA does improve $CdSe_{(s)}$ dissolution rates, EDTA is not the sole factor that dictates $CdSe_{(s)}$ longevity. In nature, metal complexing ligands are expected to significantly enhance QD dissolution and shorten their lifetime as nanocrystals.

The product layer control model resulted in higher R^2 values for both Zn^{2+} and Cd^{2+} data when EDTA was 0 and 0.001 mM, but as EDTA concentration increased to 0.01 and 0.1 mM, both the reaction control model and product layer diffusion model yielded similar R^2 values (Table S2). Complexation of EDTA with Cd^{2+}, Zn^{2+}, and degradation products on the QD surface and their dissolution might lower the effect of product layer diffusion limitation. Hence, the release of both Zn^{2+} and Cd^{2+} in the presence of higher EDTA concentrations can be considered to be acting under some diffusion limitation but not far from being controlled by the surface reaction.

2.5.2. *Effect of NOM*

NOM was used to evaluate whether natural organic compounds with metal chelating ability can influence the long-term dissolution of CdSe/ZnS-MPA QDs. Suwannee river NOM had minimal effect on QD core dissolution in the dark (Fig. 8). Although Cd^{2+} started leaching out earlier in the first 7 days in the presence of 10 or 50 ppm NOM compared to no

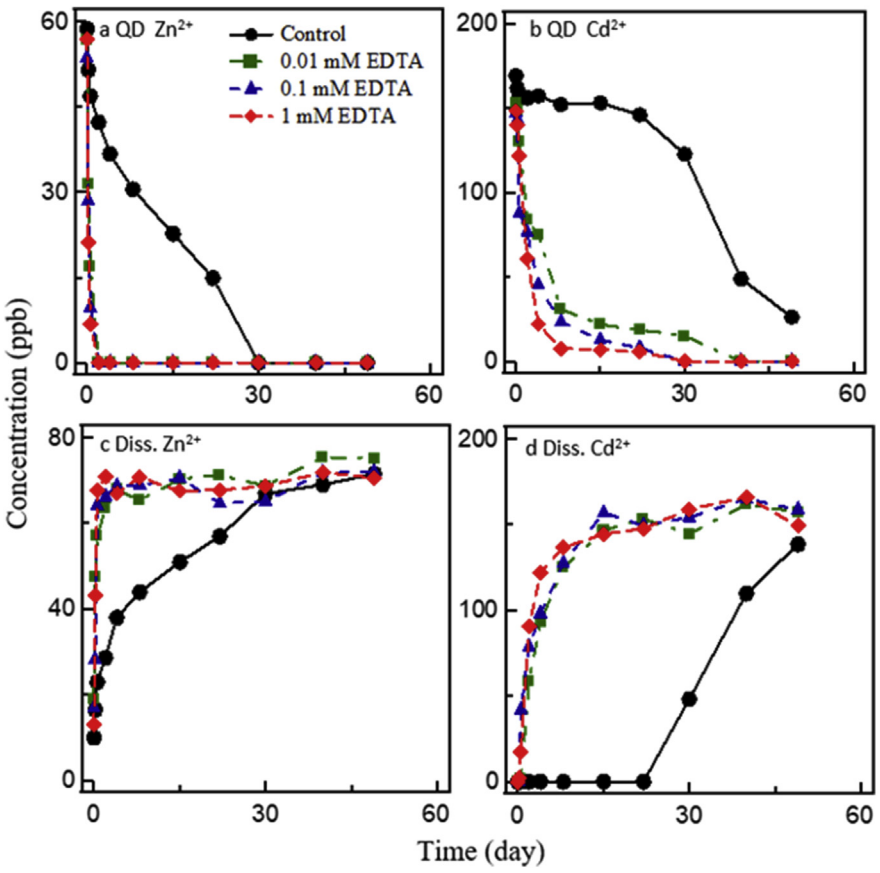

Fig. 7 – Influence of added dissolved ethylenediaminetetraacetate (EDTA) (0, 0.01, 0.1, or 1 mM) on dissolution kinetics of CdSe/ZnS QDs at pH 7. (a) Zn^{2+} in the QD phase, (b) Cd^{2+} concentrations in the QD phase, (c) dissolved Zn^{2+} concentrations, and (d) dissolved Cd^{2+} concentrations.

NOM, Cd^{2+} concentrations remained similar and within statistical significance among all batch reactors from about 20 days to 80 days. The early Cd^{2+} leaching could indicate slightly faster ZnS shell deterioration in the presence of NOM or a Cd-complexation ability of NOM. Zn^{2+} measurement was not possible since samples were swamped with Zn^{2+} ions after collection from batch reactors and prior to centrifugation to increase Cd^{2+} recovery in the centrifugal ultra-filtration process.

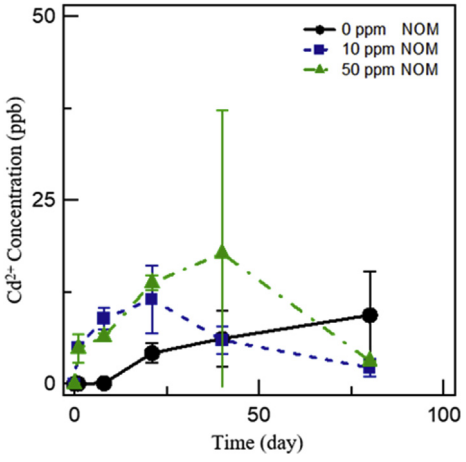

Fig. 8 – Concentration of dissolved Cd^{2+} leached from CdSe/ZnS QDs over time in the presence of Suwannee River natural organic matter (0, 10 and 50 ppm) at pH 6.5.

Humic substances can affect environmental transformations of QDs (Slaveykova and Startchev, 2009; Navarro et al., 2010; Li et al., 2012; Quigg et al., 2013; Chang and Waclawik, 2014). Humic substances can transform surface properties of the QDs by covering their surfaces or displacement of the capping groups (Navarro et al., 2010; Liu et al., 2012). This impacts QDs aggregation (Buffle et al., 1998; Slaveykova and Startchev, 2009; Zhang et al., 2012a) or can cause change in their dispersibility and transfer within different medias (Navarro et al., 2010; Celiz et al., 2011). However, no change in QDs dissolution extent and rate in the presence of the humic substances and in the dark has been previously observed. Celiz et al. exposed carboxylic and amine polyethylene glycol (PEG)-functionalized CdSe/ZnS QDs to Suwannee river humic and fulvic acids in dark and with QD:HS mole ratios up to 1:1000 and observed no Cd^{2+} ions in the solution after 24 h of exposure time (Celiz et al., 2011). Xiao et al. experimented with 0.1 and 0.3 ppm of CdSe–COOH and CdSe-PDDA QDs in the presence of 20 ppm humic acid and observed that in limited light conditions QDs dissolution was not affected by humic acid presence, over the 30 day experimental period (Xiao et al., 2016). These studies are in agreement with our results of no lasting influence of dissolved

organic matter on QD dissolution extent after 3 month of exposure time. Although HA or NOM might not promote QD dissolution, It could act as a complexing ligand to sequester Cd^{2+} after QD dissolution. It has been observed that amounts as low as 5 mg/L (1 mM) of HA and 1 mg/L (15 nM) of bovine serum albumin decrease the free Cd and Se concentrations (Mahendra et al., 2008). Subsequent ligand-Cd^{2+} complexation could reduce bioavailability of the Cd^{2+} free ions and thus QDs toxicity.

2.6. QD concentration effect

QD homo-aggregation may affect their stability and behavior in water (Mulvihill et al., 2010; Xiao et al., 2016; Zhang et al., 2008b). Aggregation has been shown to have a preservation effect on metallic nanoparticles and decrease both dissolution rates and extents (Hotze et al., 2010; Liu et al., 2008; Vikesland et al., 2007; Zhang et al., 2012a). Here, aggregate formation was examined for any ability to slow dissolution rates of CdSe/ZnS-MPA capped QDs. QD aggregation may be important when QDs are released into the waste streams or from products as aggregates, or when aqueous conditions such as high ionic strength, presence of bridging cations, or loss of capping agent (Morelli et al., 2012; Noh et al., 2010; Xiao et al., 2016; Zhang et al., 2008b) promote aggregation.

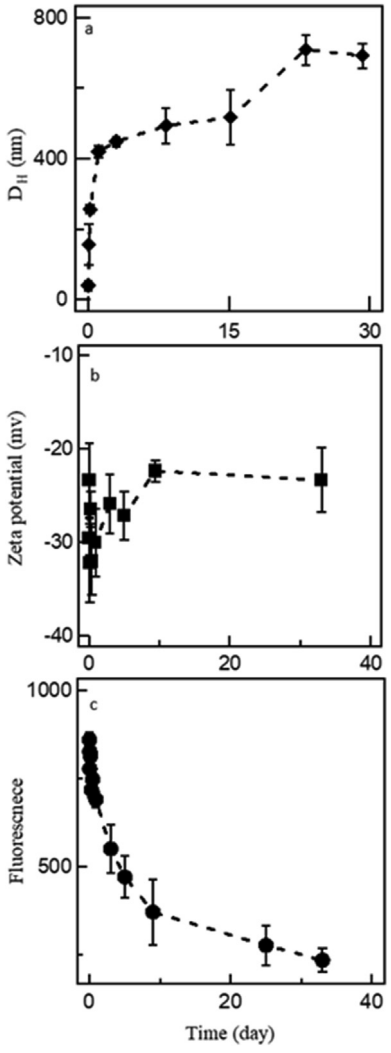

Fig. 9 – (a) Hydrodynamic diameter, (b) zeta potential, and (c) fluorescence of 20 ppm MPA-capped CdSe/ZnS QDs over time.

Dynamic light scattering measurements showed an increase from 25 nm to around 700 nm in QD hydrodynamic diameter (D_h) after a month, indicating QD aggregation occurred in a suspension of 20 ppm QDs (Fig. 9a). D_h showed a rapid increase during the first hours to over 400 nm, and incremental increase in size was more gradual afterwards. Surprisingly, almost no dissolution of a 20 ppm QD suspension was observed during the entire time course. After 30 days, dissolved Zn^{2+} concentration was 2 ppb, and dissolved Cd concentration was <1 ppb. Two other physicochemical measurements of QDs in suspension also supported no chemical transformation. Zeta potential measurements (Fig. 9b) and spectrofluorescence measurements (Fig. 9c) also supported no observable chemical transformation. Zeta potential started at −29.5 ± 10.2 mV and remained statistically the same after 30 days at −23.3 ± 3.4 mV, with only a slight decrease and recovery in the first few days. Should significant QD dissolution and metals leaching occur, concurrent release of the negatively charged MPA capping agent should also happen, leading to a less negative surface charge, which was not observed. Peak spectrofluorescence intensity decreased overtime, while no shift in the peak location (i.e. red shift or blue shift) was observed, indicating that no measurable core size change has happened. The fluorescence quenching over time can be explained by aggregation of the QDs which blocks inner QDs from light interactions or fluorescence (Noh et al., 2010).

QDs dissolution was therefore strongly inhibited when high concentrations of QDs were present. A similar preservation effect has been observed previously for other nanoparticles (Hotze et al., 2010; Liu et al., 2008; Vikesland et al., 2007; Zhang et al., 2012a). Liu et al. studied dissolution of lead sulfide (PbS) nanoparticles (Liu et al., 2008) and observed that the dissolution rate of 240 nm aggregates of PbS (4.7×10^{-10} mol $m^{-2}s^{-1}$) was an order of magnitude lower than for monodisperse 14 nm PbS (4.4×10^{-9} mol m^{-2} s^{-1}). The authors attributed this decrease in dissolution rate and extent to three possible reasons: decrease in available surface area for dissolution as a result of aggregation, increase in water viscosity in the highly confined space between the particles in the aggregates, and the overlap of the diffusion layer between two particles in an aggregate which can lower the concentration gradient and thus the driving force for dissolution. For the commercial QDs studied here, the higher concentration of QDs (20 ppm) was also likely accompanied by a higher concentration of excess dissolved MPA as provided by the supplier, compared to the 1 ppm QD suspensions above. As discussed in section 2.2, the excess dissolved capping agent can temporarily inhibit QD dissolution. Lower dissolution rate and extent of aggregate size compared to monodispersed QDs could play an important role in their stability in the environment. Larger aggregate size may prolong their stability and might increases their longevity before complete dissolution.

2.7. Toxicity of QDs with ageing

Growth of *E. coli* was used as a surrogate indicator of metal-induced toxicity of whole QDs and dissolved QDs. *E. coli* cells were exposed to either in-tact QDs, partially dissolved QDs, or fully dissolved QDs at similar concentrations used in dissolution experiments above (Fig. 10). The presence of no QD amendments showed the fastest and greatest extent of growth, but additions of metals resulted in somewhat slower growth and to lesser extents after 9 h. The most growth inhibition occurred when either in-tact QDs or partially dissolved QDs were present, and fully dissolved QDs appeared to produce only a slight decrease in growth. The differences in growth extent after 9 h with and without metals is somewhat small and likely due to the low concentrations of metals used here (1 ppm QDs) as opposed to much higher concentrations used in other toxicity studies (75 ppm QDs) (Priester et al., 2009). Nevertheless, the final OD_{600} values with QDs are statistically significant (at $p = 0.01$), and dissolved metals present are statistically significant (at $p = 0.05$) from those without added metals.

The CdSe/ZnS QDs at low concentrations used here are therefore considered to have a greater toxic influence on *E. coli* compared to fully dissolved metals alone. This observation is consistent with some toxicity studies having found QDs causing a greater toxic effect compared to leached metals, in particular for higher organisms (Buffet et al., 2015; Hsu et al., 2012; Priester et al., 2009; Zhang et al., 2012b). However, others with aquatic organisms and microorganisms indicate toxic responses are due primarily to leached Cd^{2+} (Derfus et al., 2004; Mahendra et al., 2008; Stewart et al., 2013). In addition to leachability, QD bioaccumulation or toxicity has been found to depend on QD properties such as surface capping agent (Pace et al., 2010; Zhang et al., 2017) and size (Pace et al., 2010). Cd within QDs and freely dissolved Cd^{2+} have shown different bioaccumulation extents in a variety of organisms (Priester et al., 2009; Domingos et al., 2011; Hsu et al., 2012; Morelli et al., 2012). Whether QD Cd^{2+} or dissolved Cd^{2+} is the greater threat to entire ecosystem health is still an open question, but their simultaneous occurrence should be expected and considered where Cd-bearing electronic waste such as QDs are introduced to the environment. Our experiments addressing QD longevity and Cd^{2+} leaching could support future toxicological studies that investigate the dual exposure routes (solid phase and dissolved phase) of QD-related metallic pollution.

2.8. Environmental and material implications

QD degradation and release of metal cations within oxic waters is thought to be governed simultaneously by oxidation of S^{2-} or Se^{2-} by O_2 and by mineral solubility. The observed slower ZnS dissolution and lack of any Cd^{2+} release under anoxic conditions compared to oxic conditions over two months confirms oxidation by O_2 as the primary transformation process in aphotic environments. Therefore anoxic environments at neutral pH such as saturated groundwater zones or other subsurface sediments could represent places

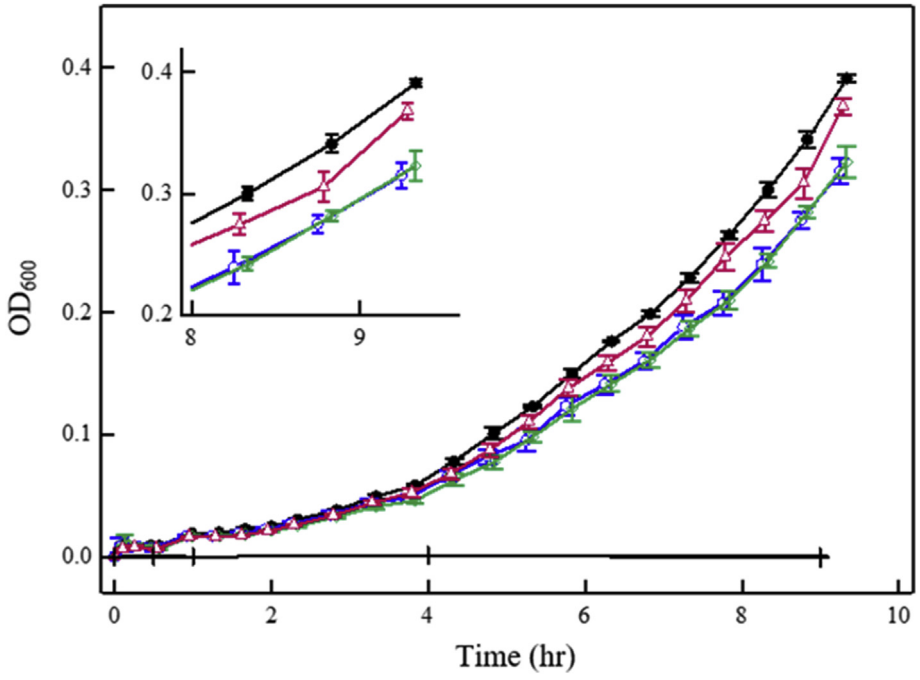

Fig. 10 – Growth rate curves of *E. coli* K12 cells at 37°C measured by optical density (OD_{600}) over time under different solution conditions: LB medium alone (black filled squares), LB medium with 1 ppm QDs (blue circles), LB medium with partially dissolved QDs (0.7 ppm QDs, 30 ppb dissolved Cd^{2+}, 24 ppb dissolved Zn^{2+}) (green diamonds), and LB medium with dissolved QDs only (150 ppb dissolved Cd^{2+}, 68 ppb dissolved Zn^{2+}, no QDs remaining) (red triangles). Measurements of three control solutions without cells (all black plus markers) overlap at or near $OD_{600} = 0.0$. Error bars represent standard deviations on measurements of triplicate reactors.

where QDs might have long lifetimes. Our results also show that QD longevity might be extended if QD pollution is accompanied by excess dissolved precursor molecules that have a suppression effect on QD mineral solubility. The addition of excess metal chelators (EDTA) significantly accelerated metal cation release and suggests biogenic complexing organic molecules (e.g., exuded organic acids or siderophores) may contribute to QD degradation. Ligand-promoted dissolution in anoxic conditions should also be tested to assess the relative contributions of O_2 and ligands. The presence of sunlight should further accelerate QD degradation through oxidation by photo-generated holes and ROS (Aldana et al., 2001; Durisic et al., 2009; Ibnaouf et al., 2014; Karakoti et al., 2011; Li et al., 2012; Morelli et al., 2012; Mulvihill et al., 2010; Siy and Bartl, 2010; Slaveykova and Startchev, 2009; Zhang et al., 2008, 2012), such as H_2O_2 as confirmed here.

The ZnS shell is not entirely protective of the CdSe core and may completely dissolve within one to a few weeks in natural waters. Moreover, Cd^{2+} was also observed to leach prior to complete ZnS disappearance, likely due to non-uniformity in ZnS coverage. More uniform coverage and greater ZnS thickness might prolong QD lifetime and slow core dissolution, as has been observed for photochemical dissolution (Grabolle et al., 2008). Furthermore, ZnS is a reactive mineral to O_2 which accelerates Zn^{2+} dissolution. A less reactive mineral such as a metal oxide or other forms of surface passivation (Lu et al., 2019) may better preserve the QD, provided the chosen shell mineral still provides the desired electronic and optical properties. The use of more insoluble transition metals, such as In or Fe, should be considered as well. A densely arranged surface organic polymer, or even graphitic shell, may offer superior protection from H_2O and O_2 intrusion.

Our understanding of dissolution rates and mechanisms for QDs possessing core-shell structures would benefit from improved kinetic models. As a first approximation, the shrinking particle kinetic model with a product layer diffusion control sufficiently modeled the CdSe/ZnS dissolution kinetics for both metal cations, although the surface reaction model seemed applicable as well under some conditions. The composition and dynamics of this product layer, should it exist, remains to be characterized with spectroscopy. Accordingly, the experiments and modeling presented here provide an indication of what chemical processes may be important if commercial QDs are released into natural waters, but further measurements at the QD-water interface are needed to characterize these surface processes. A kinetic model that improves on these uncertainties needs to be developed and could include all the processes of product layer evolution, shell dissolution, and time-delayed core dissolution.

Future studies should also address how to quantify aggregation effects on QD dissolution. Our results show that QD aggregates could probably reside in water for longer periods compared to monodispersed particles. QD homoaggregation may be important when QDs are released into the waste streams or from products as homoaggregates, or when aqueous conditions such as high ionic strength, presence of bridging cations, or loss of capping agent (Morelli et al., 2012; Noh et al., 2010; Xiao et al., 2016; Zhang et al., 2008b) promote aggregation. In nature, heteroaggregation of QDs may be a more important process due to the greater abundance of suspended clays, silts, insoluble organic matter, or biocolloids compared to released nanomaterial concentrations (Lowry et al., 2012; Praetorius et al., 2014). Heteroaggregation should influence QD reactivity by decreasing available surface area to dissolution or photodegradation, and substrate surfaces could act as a sink for dissolved metals. Others (Al-Salim et al., 2011) have recognized the dearth of information on QD heteroaggregation with soil components, and QD behavior in metals remediation of soil requires further study (Ye et al., 2017b). Further experimentation is necessary to characterize attachment efficiencies to natural colloids or soil components. Any potential role of NOM on QD dissolution or (dis)aggregation remains less clear, however. QDs are susceptible to enhanced dispersion by NOM coating QD surfaces and stabilizing them in water (Mahendra et al., 2008; Slaveykova and Startchev, 2009; Navarro et al., 2010; Celiz et al., 2011), but how this affects dissolution still requires further study.

3. Conclusions

This study aimed to investigate important water chemistry factors that control the dissolution of CdSe/ZnS-MPA capped QDs in aquatic environments. Dissolved and solid-phase Zn^{2+} and Cd^{2+} concentrations were monitored for 30–80 days for CdSe/ZnS-MPA QDs subjected to a variety of water chemistries. Our data shows that at neutral pH and in the absence of dissolved oxygen, strong chelating agents, oxidants, and light, the CdSe/ZnS QDs are slow dissolve, with progressive ZnS dissolution over weeks and the core CdSe mineral remaining solid for over two months. The chemical resistance of CdSe even at a few nm in size gives it significant time for movement among environmental compartments and exposure to aquatic life as a nanoparticle. Dissolved oxygen was indicated as the most important water chemistry factor in QD dissolution, as ZnS dissolution rates were significantly slowed in the absence of O_2 and accompanied by no CdSe dissolution. Furthermore additional oxidants (here, H_2O_2) further facilitated dissolution. Therefore oxidation of solid phase S^{2-} and Se^{2-} is likely an important step in QD degradation. Mineral solubility was also found to influence dissolution rates for QDs under oxic conditions. The addition of dissolved excess QD precursors including Cd^{2+}, Zn^{2+}, and MPA temporarily slowed CdSe/ZnS-MPA degradation consistent with mineral-water equilibria. In contrast, the presence complexing ligands (here, EDTA) significantly increased dissolution rates by increasing metal cation solubility. The role of dissolved NOM in influencing QD dissolution, however, was not clearly identified. Kinetic modeling revealed that accumulation of a product layer may limit metal leaching rates, but removal of this product layer may shift dissolution to reaction control. Overall, these results support the assumption that few nanometer sized mineral phases may have a shorter lifetime in natural waters compared to their bulk mineral counterparts.

Declaration of Competing Interest

The authors declare that they have no known competing financial interests or personal relationships that could have appeared to influence the work reported in this paper.

Acknowledgments

This work was financially supported by the United States National Science Foundation (grant number CBET-1254245). The authors thank the Core Mass Spectrometry Facility at Northeastern University for laboratory support. The authors also thank Annalisa Onnis-Hayden, Ameet Pinto, Katherine Vilardi, and Nazli Rafei Dehkordi for assistance with bacteria growth.

Appendix A. Supplementary data

Supplementary data to this article can be found online at https://doi.org/10.1016/j.jes.2019.11.011.

REFERENCES

Acero, P., Cama, J., Ayora, C., 2007. Sphalerite dissolution kinetics in acidic environment. Appl. Geochem. 22, 1872–1883.
Al-Salim, N., Barraclough, E., Burgess, E., Clothier, B., Deurer, M., Green, S., et al., 2011. Quantum dot transport in soil, plants, and insects. Sci Total Environ 409, 3237–3248.
Aldana, J., Lavelle, N., Wang, Y., Peng, X., 2005. Size-dependent dissociation pH of thiolate ligands from cadmium chalcogenide nanocrystals. J. Am. Chem. Soc. 127, 2496–2504.
Aldana, J., Wang, Y.A., Peng, X., 2001. Photochemical instability of CdSe nanocrystals coated by hydrophilic thiols. J. Am. Chem. Soc. 123, 8844–8850.
Alivisatos, A.P., 1996. Perspectives on the physical chemistry of semiconductor nanocrystals. J. Phys. Chem. 100, 13226–13239.
Alivisatos, P., 2004. The use of nanocrystals in biological detection. Nat. Biotechnol. 22, 47–52.
Aydogan, S., 2006. Dissolution kinetics of sphalerite with hydrogen peroxide in sulphuric acid medium. Chem. Eng. J. 123, 65–70.
Ballou, B., Lagerholm, B.C., Ernst, L.A., Bruchez, M.P., Waggoner, A.S., 2004. Noninvasive imaging of quantum dots in mice. Bioconjug. Chem. 15, 79–86.
Buffet, P.E., Zalouk-Vergnoux, A., Poirier, L., Lopes, C., Risso-de-Faverney, C., Guibbolini, et al., 2015. Cadmium sulfide quantum dots induce oxidative stress and behavioral impairments in the marine clam Scrobicularia plana. Environ. Toxicol. Chem. 34, 1659–1664.
Buffle, J., Wilkinson, K.J., Stoll, S., Zhang, J., 1998. A generalized description of aquatic colloidal interactions : The three-colloidal component approach. Environ. Sci. Technol. 32, 2887–2899.
Celiz, M.D., Colón, L. a, Watson, D.F., Aga, D.S., 2011. Study on the effects of humic and fulvic acids on quantum dot nanoparticles using capillary electrophoresis with laser-induced fluorescence detection. Environ. Sci. Technol. 45, 2917–2924.
Chang, J., Waclawik, E.R., 2014. Colloidal semiconductor nanocrystals: controlled synthesis and surface chemistry in organic media. RSC Adv 4, 23505–23527.
Cooper, W.J., Lean, D.R.S., 1989. Hydrogen peroxide concentration in a northern lake: Photochemical formation and diel variability. Environ. Sci. Technol. 23, 1425–1428.
Cooper, W.J., Zika, R.G., Petasne, R.G., Plane, J.M.C., 1988. Photochemical formation of H_2O_2 in natural waters exposed to sunlight. Environ. Sci. Technol. 22, 1156–1160.
Crundwell, F.K., Verbaan, B., 1987. Kinetics and mechanisms of the non-oxidative dissolution of sphalerite. Hydrometallurgy 17, 369–384.
Dabbousi, B.O., Rodriguez, J., Mikulec, F.V., Heine, J.R., Mattoussi, H., Ober, R., et al., 1997. (CdSe)ZnS Core - Shell quantum dots : Synthesis and characterization of a size series of highly luminescent nanocrystallites. J. Phys. Chem. B 101, 9463–9475.
Derfus, A.M., Chan, W.C.W., Bhatia, S.N., 2004. Probing the cytotoxicity of semiconductor quantum dots. Nano Lett 4, 11–18.
Domingos, R.F., Simon, D.F., Hauser, C., Wilkinson, K.J., 2011. Bioaccumulation and effects of CdTe/CdS quantum dots on chlamydomonas reinhardtii - Nanoparticles or the free ions? Environ. Sci. Technol. 45, 7664–7669.
Durisic, N., Godin, A.G., Walters, D., Grütter, P., Wiseman, P.W., Heyes, C.D., 2011. Probingthe "dark" fraction of core-shell quantum dots by ensemble and single particle pH-dependent spectroscopy. ACS Nano 5, 9062–9073.
Durisic, N., Wiseman, P.W., Grütter, P., Heyes, C.D., 2009. A common mechanism underlies the dark fraction formation and fluorescence blinking of quantum dots. ACS Nano 3, 1167–1175.
Fujii, M., Otani, E., 2017. Photochemical generation and decay kinetics of superoxide and hydrogen peroxide in the presence of standard humic and fulvic acids. Water Res 123, 642–654.
Ghassa, S., Noaparast, M., Shafaei, S.Z., Abdollahi, H., Gharabaghi, M., Boruomand, Z., 2017. A study on the zinc sulfide dissolution kinetics with biological and chemical ferric reagents. Hydrometallurgy 171, 362–373.
Grabolle, M., Ziegler, J., Merkulov, A., Nann, T., Resch-Genger, U., 2008. Stability and fluorescence quantum yield of CdSe-ZnS quantum dots - Influence of the thickness of the ZnS shell. Ann. N. Y. Acad. Sci. 1130, 235–241.
Green, M., 2010. The nature of quantum dot capping ligands. J. Mater. Chem. 20, 5797–5809.
Gustafsson, J.P., 2018. Visual Minteq v.3.1. 2018. Available: https://vminteq.lwr.kth.se/. (Accessed 2 February 2014).
Habashi, F., 1966. The mechanism of oxidation of sulfide ores in nature. Econ. Geol. 61, 587–591.
Hardman, R., 2006. A toxicologic review of quantum dots: Toxicity depends on physicochemical and environmental factors. Environ. Health Perspect. 114, 165–172.
Hider, R.C., Kong, X., 2010. Chemistry and biology of siderophores. Nat. Prod. Rep. 27, 637.
Hotze, E.M., Phenrat, T., Lowry, G.V., 2010. Nanoparticle aggregation: Challenges to understanding transport and reactivity in the environment. J. Environ. Qual. 39, 1909.
Hsieh, Y.H., Huang, C.P., Davis, A.P., 1993. Photo-oxidative dissolution of CdS(s): The effect of Pb(II) ions. Chemosphere 27, 721–732.
Hsu, P.C.L., O'Callaghan, M., Al-Salim, N., Hurst, M.R.H., 2012. Quantum dot nanoparticles affect the reproductive system of Caenorhabditis elegans. Environ. Toxicol. Chem. 31, 2366–2374.
Hu, L., Zhang, C., Zeng, G., Chen, G., Wan, J., Guo, Z., et al., 2016. Metal-based quantum dots: Synthesis, surface modification, transport and fate in aquatic environments and toxicity to microorganisms. RSC Adv 6, 78595–78610.

Ibnaouf, K.H., Prasad, S., Al Salhi, M.S., Hamdan, A., Zaman, M.B., El Mir, L., 2014. Influence of the solvent environments on the spectral features of CdSe quantum dots with and without ZnS shell. J. Lumin. 149, 369–373.
Ipe, B.I., Lehnig, M., Niemeyer, C.M., 2005. On the generation of free radical species from quantum dots. Small 1, 706–709.
Karakoti, A.S., Sanghavi, S., Nachimuthu, P., Yang, P., Thevuthasan, S., 2011. Probing the size- and environment-induced phase transformation in CdSe quantum dots. J. Phys. Chem. Lett. 2, 2925–2929.
Klaine, S.J., Alvarez, P.J.J., Batley, G.E., Fernandes, T.F., Handy, R.D., Lyon, D.Y., et al., 2008. Nanomaterials in the environment: behavior, fate, bioavailability, and effects. Environ. Toxicol. Chem. 27, 1825–1851.
Lazo, D.E., Dyer, L.G., Alorro, R.D., 2017. Silicate, phosphate and carbonate mineral dissolution behaviour in the presence of organic acids: A review. Miner. Eng. 100, 115–123.
Levenspiel, O., 1999. Chemical Reaction Engineering, third ed. John Wiley & Sons, New York.
Li, Y., Zhang, W., Li, K., Yao, Y., Niu, J., Chen, Y., 2012. Oxidative dissolution of polymer-coated CdSe/ZnS quantum dots under UV irradiation: Mechanisms and kinetics. Environ. Pollut. 164, 259–266.
Liu, J., Aruguete, D.M., Jinschek, J.R., Donald Rimstidt, J., Hochella, M.F., 2008. The non-oxidative dissolution of galena nanocrystals: Insights into mineral dissolution rates as a function of grain size, shape, and aggregation state. Geochim. Cosmochim. Acta 72, 5984–5996.
Liu, J., Katahara, J., Li, G., Coe-Sullivan, S., Hurt, R.H., 2012. Degradation products from consumer nanocomposites: A case study on quantum dot lighting. Environ. Sci. Technol. 46, 3220–3227.
Lowry, G.V., Gregory, K.B., Apte, S.C., Lead, J.R., 2012. Transformations of nanomaterials in the environment. Environ. Sci. Technol. 46, 6893–6899.
Lu, H., Carroll, G.M., Neale, N.R., Beard, M.C., 2019. Infrared quantum dots: Progress, challenges, and opportunities. ACS Nano 13, 939–953.
Luque, A., Martí, A., Nozik, A.J., 2007. Solar cells based on quantum dots: Multiple exciton generation and intermediate bands. MRS Bull 32, 236–241.
Mahendra, S., Zhu, H., Colvin, V.L., Alvarez, P.J., 2008. Quantum dot weathering results in microbial toxicity. Environ. Sci. Technol. 42, 9424–9430.
Mandai, A., Tamai, N., 2008. Influence of acid on luminescence properties of thioglycolic acid-capped CdTe quantum dots. J. Phys. Chem. C 112, 8244–8250.
Marschner, H., Römheld, V., Kissel, M., 1986. Different strategies in higher plants in mobilization and uptake of iron. J. Plant Nutr. 9, 695–713.
Morelli, E., Cioni, P., Posarelli, M., Gabellieri, E., 2012. Chemical stability of CdSe quantum dots in seawater and their effects on a marine microalga. Aquat. Toxicol. 122–123, 153–162.
Mulvihill, M.J., Habas, S.E., Jen-La Plante, I., Wan, J., Mokari, T., 2010. Influence of size, shape, and surface coating on the stability of aqueous suspensions of CdSe nanoparticles. Chem. Mater. 22, 5251–5257.
Navarro, D.A., Banerjee, S., Aga, D.S., Watson, D.F., 2010. Partitioning of hydrophobic CdSe quantum dots into aqueous dispersions of humic substances: Influence of capping-group functionality on the phase-transfer mechanism. J. Colloid Interface Sci. 348, 119–128.
Navarro, D.A., Bisson, M.A., Aga, D.S., 2012. Investigating uptake of water-dispersible CdSe/ZnS quantum dot nanoparticles by *Arabidopsis thaliana* plants. J. Hazard. Mater. 211–212, 427–435.
Noh, M., Kim, T., Lee, H., Kim, C.K., Joo, S.W., Lee, K., 2010. Fluorescence quenching caused by aggregation of water-soluble CdSe quantum dots. Colloids Surfaces A Physicochem. Eng. Asp. 359, 39–44.
Nozik, A.J., 2002. Quantum dot solar cells. Phys. E Low-Dimens. Syst Nanostruct. 14, 115–120.
Pace, H.E., Lesher, E.K., Ranville, J.F., 2010. Influence of stability on the acute toxicity of CdSe/ZnS nanocrystals to daphnia magna. Environ. Toxicol. Chem. 29, 1338–1344.
Parak, W.J., Gerion, D., Pellegrino, T., Zanchet, D., Micheel, C., Williams, S.C., et al., 2003. Biological applications of colloidal nanocrystals. Nanotechnology 14, R15–R27.
Paydary, P., Larese-casanova, P., 2015. Separation and quantification of quantum dots and dissolved metal cations by size exclusion chromatography – ICP-MS. Int. J. Environ. Anal. Chem. 95, 1450–1470.
Pechstedt, K., Whittle, T., Baumberg, J., Melvin, T., 2010. Photoluminescence of colloidal CdSe/ZnS quantum dots : The critical effect of water molecules. J.;Phys.Chem.C 114, 12069–12077.
Petosa, A.R., Jaisi, D.P., Quevedo, I.R., Elimelech, M., Tufenkji, N., 2010. Aggregation and deposition of engineered nanomaterials in aquatic environments: Role of physicochemical interactions. Environ. Sci. Technol. 44, 6532–6549.
Praetorius, A., Labille, J., Scheringer, M., Thill, A., Hungerbühler, K., Bottero, J., 2014. Heteroaggregation of titanium dioxide nanoparticles with model natural colloids under environmentally relevant conditions. Environ. Sci. Technol. 48, 10690–10698.
Priester, J.H., Stoimenov, P.K., Mielke, R.E., Webb, S.M., Ehrhardt, C., Zhang, J.P., et al., 2009. Effects of soluble cadmium salts versus cdse quantum dots on the growth of planktonic pseudomonas aeruginosa. Environ. Sci. Technol. 43, 2589–2594.
Quevedo, I.R., Tufenkji, N., 2009. Influence of solution chemistry on the deposition and detachment kinetics of a CdTe quantum dot examined using a quartz crystal microbalance. Environ. Sci. Technol. 43, 3176–3182.
Quigg, A., Chin, W., Chen, C., Zhang, S.-J., Jiang, Y., Miao, A., et al., 2013. Direct and indirect toxic effects of engineered nanoparticles on algae: Role of natural organic matter. Sustain. Chem. Eng. 1, 686–702.
Siy, J.T., Bartl, M.H., 2010. Insights into reversible dissolution of colloidal CdSe nanocrystal quantum dots. Chem. Mater. 22, 5973–5982.
Slaveykova, V.I., Startchev, K., 2009. Effect of natural organic matter and green microalga on carboxyl-polyethylene glycol coated CdSe/ZnS quantum dots stability and transformations under freshwater conditions. Environ. Pollut. 157, 3445–3450.
Spanhel, L., Haase, M., Weller, H., Henglein, A., 1987. Photochemistry of colloidal semiconductors. 20. Surface modification and stability of strong luminescing CdS particles. J. Am. Chem. Soc. 109, 5649–5655.
Stewart, D.T.R., Noguera-Oviedo, K., Lee, V., Banerjee, S., Watson, D.F., Aga, D.S., 2013. Quantum dots exhibit less bioaccumulation than free cadmium and selenium in the earthworm Eisenia andrei. Environ. Toxicol. Chem. 32, 1288–1294.
Van Sark, W.G.J.H.M., Frederix, P.L.T.M., Van den Heuvel, D.J., Gerritsen, H.C., Bol, A.A., Van Lingen, J.N.J., et al., 2001. Photooxidation and photobleaching of single CdSe/ZnS quantum dots probed by room-temperature time-resolved spectroscopy. J. Phys. Chem. B 105, 8281–8284.
Vančura, V., Hovadík, A., 1965. Root exudates of plants II. Composition of root exudates of some vegetables. Plant Soil 22, 21–32.
Vikesland, P.J., Heathcock, A.M., Rebodos, R.L., Makus, K.E., 2007. Particle size and aggregation effects on magnetite reactivity

toward carbon tetrachloride. Environ. Sci. Technol. 41, 5277–5283.
Wu, P., Zhao, T., Wang, S., Hou, X., 2014. Semicondutor quantum dots-based metal ion probes. Nanoscale 6, 43–64.
Xiao, Y., Ho, K.T., Burgess, R.M., Cashman, M., 2016. Aggregation, sedimentation, dissolution, and bioavailability of quantum dots in estuarine systems. Environ. Sci. Technol. 51, 1357–1363.
Yang, Y., Zhu, H., Colvin, V.L., Alvarez, P.J., 2011. Cellular and transcriptional response of pseudomonas stutzeri to quantum dots under aerobic and denitrifying conditions. Environ. Sci. Technol. 45, 4988–4994.
Ye, S., Zeng, G., Wu, H., Zhang, C., Liang, J., Dai, J., et al., 2017a. Co-occurrence and interactions of pollutants, and their impacts on soil remediation-A review. Crit. Rev. Env. Sci. Tec. 47, 1528–1553.
Ye, S., Zeng, G., Wu, H., Zhang, C., Dai, J., Liang, J., et al., 2017b. Biological technologies for the remediation of co-contaminated soil. Crit. Rev. Biotechnol. 37, 1062–1076.
Ye, S., Yan, M., Tan, X., Liang, J., Zeng, G., Wu, H., et al., 2019a. Facile assembled biochar-based nanocomposite with improved graphitization for efficient photocatalytic activity driven by visible light. Appl. Catal. B-Environ. 250, 78–88.
Ye, S., Zeng, G., Wu, H., Liang, J., Zhang, C., Dai, J., et al., 2019b. The effects of activated biochar addition on remediation efficiency of co-compositing with contaminated wetland soil. Resour. Conserv. Recy. 140, 278–285.
Zeng, C., Ramos-Ruiz, A., Field, J.A., Sierra-Alvarez, R., 2015. Cadmium telluride (CdTe) and cadmium selenide (CdSe) leaching behavior and surface chemistry in response to pH and O_2. J. Environ. Manage. 154, 78–85.
Zhang, H., Chen, B., Banfield, J.F., 2010. Particle size and pH effects on nanoparticle dissolution. J. Phys. Chem. C 114, 14876–14884.
Zhang, M., Wei, X., Ding, L., Hu, J., Jiang, W., 2017. Adhesion of CdTe quantum dots on model membranes and internalization into RBL-2H3 cells. Environ. Pollut. 225, 419–427.
Zhang, S., Jiang, Y., Chen, C.S., Spurgin, J., Schwehr, K.A., Quigg, A., et al., 2012a. Aggregation, dissolution, and stability of quantum dots in marine environments: Importance of extracellular polymeric substances. Environ. Sci. Technol. 46, 8764–8772.
Zhang, W., Lin, K., Miao, Y., Dong, Q., Huang, C., Wang, H., et al., 2012b. Toxicity assessment of zebrafish following exposure to CdTe QDs. J. Hazard. Mater. 213–214, 413–420.
Zhang, Yang, Chen, Y., Westerhoff, P., Crittenden, J.C., 2008a. Stability and removal of water soluble CdTe quantum dots in water. Environ. Sci. Technol. 42, 321–325.
Zhang, Yu, Mi, L., Wang, P.N., Ma, J., Chen, J.Y., 2008b. pH-dependent aggregation and photoluminescence behavior of thiol-capped CdTe quantum dots in aqueous solutions. J. Lumin. 128, 1948–1951.
Zhao, D.L., Chung, T.-S., 2018. Applications of carbon quantum dots (CQDs) in membrane technologies: A review. Wat. Res. 147, 43–49.